



RESEARCH ARTICLE

Cannabidiol inhibits SARS-Cov-2 spike (S) protein-induced cytotoxicity and inflammation through a PPAR γ -dependent TLR4/NLRP3/Caspase-1 signaling suppression in Caco-2 cell line

Chiara Corpetti¹ | Alessandro Del Re¹ | Luisa Seguella^{1,2} | Irene Palenca¹ | Sara Rurgo³ | Barbara De Conno³ | Marcella Pesce³  | Giovanni Sarnelli³ | Giuseppe Esposito¹ 

¹Department of Physiology and Pharmacology, Sapienza University of Rome, Rome, Italy

²Department of Physiology, Michigan State University, East Lansing, Michigan, USA

³Department of Clinical Medicine and Surgery, University of Naples "Federico II", Naples, Italy

Correspondence

Giuseppe Esposito, Department of Physiology and Pharmacology "V. Erspamer", Sapienza University of Rome, P.le A. Moro, 5, 00185 Rome, Italy.

Email: giuseppe.esposito@uniroma1.it

Given the abundance of angiotensin converting enzyme 2 (ACE-2) receptors density, beyond the lung, the intestine is considered as an alternative site of infection and replication for severe acute respiratory syndrome by coronavirus type 2 (SARS-CoV-2). Cannabidiol (CBD) has recently been proposed in the management of coronavirus disease 2019 (COVID-19) respiratory symptoms because of its anti-inflammatory and immunomodulatory activity exerted in the lung. In this study, we demonstrated the in vitro PPAR- γ -dependent efficacy of CBD (10^{-9} - 10^{-7} M) in preventing epithelial damage and hyperinflammatory response triggered by SARS-CoV-2 spike protein (SP) in a Caco-2 cells. Immunoblot analysis revealed that CBD was able to reduce all the analyzed proinflammatory markers triggered by SP incubation, such as toll-like receptor 4 (TLR-4), ACE-2, family members of Ras homologues A-GTPase (RhoA-GTPase), inflammasome complex (NLRP3), and Caspase-1. CBD caused a parallel inhibition of interleukin 1 beta (IL-1 β), IL-6, tumor necrosis factor alpha (TNF- α), and IL-18 by enzyme-linked immunosorbent assay (ELISA) assay. By immunofluorescence analysis, we observed increased expression of tight-junction proteins and restoration of transepithelial electrical resistance (TEER) following CBD treatment, as well as the rescue of fluorescein isothiocyanate (FITC)-dextran permeability induced by SP. Our data indicate, in conclusion, that CBD is a powerful inhibitor of SP protein enterotoxicity in vitro.

KEYWORDS

Caco-2, Cannabidiol, NLRP3, SARS-CoV-2 spike (S) protein

1 | INTRODUCTION

The ongoing pandemic due to severe acute respiratory syndrome coronavirus 2 (SARS-CoV-2) has led to unprecedented challenges for

the healthcare systems worldwide (Chung et al., 2021). SARS-CoV-2 is a *beta-coronavirus*, with a positive-sense single RNA filament of nearly 30kb in length, able to infect through a mechanism mediated by the viral transmembrane spike glycoprotein (SP), consisting of two

This is an open access article under the terms of the Creative Commons Attribution-NonCommercial-NoDerivs License, which permits use and distribution in any medium, provided the original work is properly cited, the use is non-commercial and no modifications or adaptations are made.

© 2021 The Authors. *Phytotherapy Research* published by John Wiley & Sons Ltd.

functional subunits, responsible for binding the host cell ACE-2 receptor (S1 subunit) and fusion of viral and cell membranes (subunit S2) (Walls et al., 2020).

In addition to its prominent pathological manifestations at respiratory and vascular level, digestive symptoms, ranging from nausea to diarrhea, have been highlighted during COVID-19 (Esposito, Pesce, Seguela, Sanseverino, Lu, Sarnelli, 2020b; Kopel et al., 2020), leading to consider the digestive tract as a potential route of infection (Zhang et al., 2020). Likewise, it has been described for other members of the *coronaviridae* family, SARS-CoV-2 is able to colonize intestinal tissue and, considering the high distribution of the ACE-2 receptors in the epithelial intestinal mucosa, to actively replicate into the gut, making this body district a crucial biological niche for SARS-CoV-2 hosting and expansion toward the respiratory and cardiovascular system (Dickson I., 2020). In addition, recent studies highlighted the ability of SARS-CoV-2 SP to interact with TLR-4 triggering an inflammatory response in both human and murine alveolar macrophages, suggesting an active role of this protein in hyperinflammatory condition-observed COVID-19 patients (Del Re et al., 2021; Zhao et al., 2021). Despite such evidence, the effects of the SARS-CoV-2 SP on the intestinal epithelial cells, on the integrity of the mucosa and its role in inflammation, are still not clearly investigated. Furthermore, as demonstrated in macrophages and in lung *epithelia*, SARS-CoV-2 SP can induce a proinflammatory response in infected cells by triggering inflammasome NLRP3 complex activation (Sebastian et al., 2021). NLRP3 protein, as part of pattern recognition receptors (PRR), is a NOD-like receptor containing the pyrin effector domain able to trigger and participate in inflammasome formation (Kelley et al., 2019). During SARS-CoV-2 infection, this pathway is hyperactivated, leading to an aberrant release of cytokines and other proinflammatory molecules at the root of cellular pyroptosis, and consequent cytokine storm that features poor prognosis in COVID-19 patients. The identification of immunomodulatory and anti-inflammatory compounds able to reduce NLRP3 activation triggered by SARS-CoV-2 SP can be regarded with particular interest especially at intestinal epithelium level. Moreover, it has been shown that the reduction of Ras homolog family members, A-GTPases (RhoA GTP) with the subsequent destruction of mosaic-like organization of the intestinal epithelium, is able to trigger the activation of NLRP3/Caspase-1/IL-1 β and IL-18 pathway (Park et al., 2016). Considering the well-established "gate-keeper" properties of CBD due to its ability to rescue RhoA GTPase (Gigli et al., 2017), we proposed it as a possible molecule able to down-regulate NLRP3/Caspase-1/IL-1 β and IL-18 pathway.

CBD is a nonpsychoactive cannabinoid from *Cannabis sativa* exerting different pharmacological activities ranging from antioxidant and anti-inflammatory to neuroprotective and immunomodulatory effects (De Filippis et al., 2011; Izzo & Sharkey, 2010). Unlike psychoactive cannabinoids such as tetrahydrocannabinol (THC), CBD does not show significant affinity to cannabinoid receptors (either CB1 and CB2), whereas, by acting on PPAR- γ (O'Sullivan & Kendall, 2010) and 5-hydroxytryptamine (5HT)-1A receptors (Mishima et al., 2005), it displays anti-inflammatory and antioxidant effects. Aside to its potent anti-inflammatory activity in the gut, acting at PPAR- γ site, CBD has

shown the ability to markedly recover epithelial mucosal damage induced various stimuli ranging from *clostridium difficile* toxin A (TcdA) (Gigli et al., 2017) to ethylenediaminetetraacetic acid (EDTA) (Alhamoruni et al., 2010) and others proinflammatory stimuli.

Although CBD's well-known anti-inflammatory and immunoregulatory activities have candidate it as a potential drug in the treatment of acute respiratory distress syndrome (ARDS) following COVID-19 infection (Bifulco et al., 2021; Nagarkatti et al., 2020), it is a possible protective effect, as well as the role of SARS-CoV-2 SP at the level of the intestine epithelium, remains obscure. To this aim, the present study focuses on investigating the effect of SARS-CoV-2 SP on NLRP3 inflammasome pathway activation and relative molecular mechanisms responsible for SARS-CoV-2 SP-induced cytotoxic damage on cultured Caco-2 cells.

2 | MATERIALS AND METHODS

Caco-2 cell line was obtained from the European Collection of Cell Cultures (ECACC, Public Health England Porton Down, Salisbury, UK). Cell culture medium, fluorescein isothiocyanate (FITC)-dextran, size 4 kDa, and 3-[4,5-dimethylthiazol-2-yl]-2,5 diphenyltetrazolium bromide (MTT) were purchased from Sigma-Aldrich (St. Louis, Missouri). The SP from SARS-CoV-2 (recombinant human novel coronavirus spike glycoprotein(S), partial (active)) was purchased by Cusabio (Wuhan, China); the purity is greater than 90%, 4',6-diamidino-2-phenylindole (DAPI) (Thermo Fisher Scientific Inc., Waltham, Massachusetts), fluorescein isothiocyanate-conjugated antirabbit antibody, and Texas red conjugated antimouse antibody were from Abcam (Cambridge, UK). CBD, the purity of which is greater than 98%, and PPAR- γ antagonist (GW9662) were purchased from Tocris Cookson, Inc. (Ballwin, Missouri). All the technical support instruments, reagents, and materials for transepithelial electrical resistance (TEER) (Merck KGaA, Darmstadt, Germany), electrophoresis, and western blot analysis were obtained from Bio-Rad (Bio-Rad Laboratories, Milan, Italy). Rabbit anti-ZO-1 and rabbit anti-TLR4 were obtained from Bioss (Bioss Antibodies, Boston), and mouse antioccludin antibody was obtained from Novus Biologicals (Minneapolis)(see Table 1,2). Mouse antiglyceraldehyde-3-phosphate dehydrogenase (GAPDH), mouse anti-RhoA-GTPase, and mouse anti-ACE-2 antibodies were purchased from Santa Cruz Biotechnology (Santa Cruz, California); rabbit anti-NLRP3 and rabbit anti-Caspase-1 were obtained from Invitrogen (Invitrogen; Thermo Fisher Scientific, Inc. Monza, Italy) (see Table 1). Enhanced chemiluminescence detection reagents were from Amersham Biosciences (Milan, Italy), and horseradish peroxidase (HRP) was obtained from Dako (Milan, Italy). The level of TNF α , IL-6, IL-1 β , and IL-18 was measured using ELISA (Section 2.7) kits.

2.1 | Cell culture

Caco-2 cells were cultured in 6-well plates in Dulbecco's Modified Eagle Medium (DMEM) containing 10% fetal bovine serum (FBS), 1%

TABLE 1 Western blot antibodies

Antibody	Host	Clonality	Dilution	Brand
Anti-TLR-4	Rabbit	Polyclonal	1:500 v/v	Bioss Antibodies, Boston, USA
Anti-ACE-2	Mouse	Monoclonal	1:300 v/v	Santa Cruz Biotechnology, CA, USA
Anti-RhoA-GTPase	Mouse	Monoclonal	5 µg/ml w/v	Santa Cruz Biotechnology, CA, USA
Anti-NLRP3	Rabbit	Polyclonal	0.4 µg/ml w/v	Invitrogen; Thermo Fisher Scientific, Inc. Monza, Italy
Anti-Caspase-1	Rabbit	Polyclonal	1:500 v/v	Invitrogen; Thermo Fisher Scientific, Inc. Monza, Italy

TABLE 2 Immunofluorescence antibodies

Antibody	Host	Clonality	Dilution	Brand
Anti-ZO-1	Mouse	Monoclonal	1:100 v/v	Bioss Antibodies, Boston, USA
Anti-occludin	Rabbit	Polyclonal	1:100 v/v	Novus Biologicals, Minneapolis, USA

penicillin–streptomycin, 2 mM L-glutamate, and 1% nonessential amino acids. A total of 1×10^6 cells/well was plated and incubated, and both undifferentiated and differentiated cells (the apical tract for TEER) were obtained at different times, depending on the assay. Cells were washed three times with phosphate-buffered saline (PBS), detached with trypsin/ethylene diamine tetraacetic acid (EDTA), and dependently on the experiment plated in 6-well plates, 96-well plates, or 10 cm diameter Petri dish and allowed to adhere for further 24 h. The Caco-2 cells were randomly divided into eight groups: 1) vehicle group, 2–4) 0.1, 1, 10 ng/ml SP group, 5–7) 10 ng/ml SP plus 10^{-9} , 10^{-8} , 10^{-7} M CBD, and 8) 10 ng/ml SP with 10^{-7} M CBD plus 9 nM GW9662 antagonist PPAR- γ . Cells were treated with SARS-CoV-2 SP dissolved in ultrapure and pyrogen-free sterile vehicle for 24 h. SP concentrations were previously selected by pilot experiment aimed at identifying the lowest effective concentration (data not shown). CBD and GW9662 were selected according to the results of previous published research (Sarnelli G. et al., 2016).

2.2 | Transepithelial electrical resistance measurement

The TEER of the Caco-2 cell monolayer was determined using the EVOM volt-ohm meter (World Precision Instruments Germany, Berlin, Germany) according to the method previously described (Wells et al., 1998). In brief, cells plated between 14 and 21 days were used, and epithelial cell layers with a TEER value greater than $1,000 \Omega/\text{cm}^2$ were considered to have tight adhesion. TEER values were measured at a current of 20 mA, corrected for background resistance value without cells, and normalized by multiplying the determined resistance by effective membrane growth area, 4.71 cm^2 . $\text{TEER} (\Omega/\text{cm}^2) = (\text{Total resistance} - \text{blank resistance}) (\Omega) \times \text{Area} (\text{cm}^2)$

2.3 | FITC–Dextran

To measure the permeability of cultured Caco-2 monolayer in our experimental conditions, we measured the flux of FITC–dextran

method (Wu et al., 2019). FITC–dextran (1 mg/ml) was then added to upper insets. Cells plated between 14 and 21 days were used; after 6 h of incubation, the basolateral medium aliquots were collected, and the fluorescence was measured at 480-nm excitation and 520-nm emission wavelengths.

2.4 | Cytotoxicity assay

The 3-[4,5-dimethylthiazol-2-yl]-2,5 diphenyltetrazolium bromide (MTT reagent) assay was used to determine Caco-2 cell proliferation and survival (Mosmann, 1983). The cells in DMEM (5×10^4 cells/well) were plated in 96-well plates and allowed to adhere for further 24 h. DMEM was then replaced with fresh medium, and the cells underwent treatments as above described, exposed to SP (0.1–10 ng/ml) alone, the highest concentration in the presence of CBD (10^{-9} – 10^{-7} M) and finally the group with 9 nM GW9662 antagonist for PPAR- γ . After 24 h, 25 µl of MTT stock solution in DMEM (5 mg/ml) were added to the cells and then incubated for 3 h at 37°C. Subsequently, the cells were lysed, and the dark blue crystals were solubilized using a 100 µl solution containing 50% N,N-dimethylformamide and 20% (w/v) sodium dodecyl sulphate (SDS) (pH 4.5). The optical density (OD) of each well was determined using a microplate spectrophotometer equipped with a 620 nm filter (PerkinElmer, Inc.; Waltham, Massachusetts).

2.5 | DNA damage in vitro evaluation

The Caco-2 undifferentiated cells were grown on glass coverslip (5×10^4 cells/well) and incubated for 24 h with DMEM; the medium was replaced with fresh medium, and the cells underwent treatments as described above. Cells were fixed with 4% PFA for 10 min and followed by three-time washing with ice-cold PBS 1X. Nonspecific binding sites were blocked by 2% bovine serum albumin (BSA). The presence of pyroptotic cells was also shown with DAPI staining. The cells were incubated with DAPI (1:50000 v/v) for 10 min and washed with PBS. The pyroptotic cells were analyzed using an inverted

immunofluorescence microscope (HBO fluorescence microscope IM-3FL4, Optika Microscope, Bergamo, Italy), and images were captured by a high-resolution digital camera (HDML 4083.13-ext 12 V 2000 mA, Optika Microscopes, Bergamo, Italy).

2.6 | Western blot analysis

Protein expression in Caco-2 cells was evaluated using Western blot analysis. Following treatments, undifferentiated cells (1×10^6 cells/well) were harvested and washed twice with ice-cold PBS by centrifugation at $180 \times g$ for 10 min at 4°C . Final cell pellet was then resuspended in a volume of $80 \mu\text{l}$ ice-cold hypotonic lysis buffer [10 mM 4-(2-hydroxyethyl)-1piperazineethanesulfonic acid (HEPES), 1.5 mM MgCl_2 , 10 mM KCl, 0.5 mM phenylmethylsulfonyl fluoride, 1.5 $\mu\text{g/ml}$ soybean trypsin inhibitor, 7 $\mu\text{g/ml}$ pepstatin A, 5 $\mu\text{g/ml}$ leupeptin, 0.1 mM benzamide, and 0.5 mM dithiothreitol (DTT)]. The suspension was rapidly passed through a syringe needle five to six times to facilitate cell lysis and centrifuged for 15 min at $13,000 \times g$ to obtain the cytoplasmic fraction. This was then diluted 1:1 with non-reducing gel loading buffer [50 mM tris(hydroxymethyl)aminomethane (tris), 10% sodium dodecyl sulfate (SDS), 10% glycerol, 2 mg bromophenol/ml], boiled for 3 min then centrifuged at $10,000 \times g$ for 10 min. The protein concentration was determined using the Bradford assay, and 50 μg proteins/lane were loaded with electrophoresis polyacrylamide mini gels. Proteins were then transferred to nitrocellulose membranes. After the transfer, the membranes were incubated with 10% nonfat dry milk in PBS overnight at 4°C and then exposed, depending on the experiments, with rabbit polyclonal anti-TLR4 (1:500 v/v), mouse monoclonal anti-ACE-2 (1:300 v/v), mouse monoclonal anti-RhoA-GTPase (5 $\mu\text{g/ml}$ p/v), rabbit polyclonal anti-NLRP3 (0.4 $\mu\text{g/ml}$ w/v), rabbit polyclonal anti-Caspase-1 (1:500 v/v), and mouse monoclonal anti-GAPDH (1:2000 v/v) according to standard experimental protocols (Table 1). Membranes were then incubated with the specific secondary antibodies conjugated to HRP. Immune complexes were exposed to enhanced chemiluminescence detection reagents, and the blots were analyzed by scanning densitometry (Versadoc MP4000; Bio-Rad, Segrate, Italy). Results were expressed as optical density (OD; arbitrary units = mm^2) and normalized against the expression of the housekeeping protein GAPDH.

2.7 | Immunofluorescence staining analysis

For these experiments, undifferentiated Caco-2 cells were cultured onto coverslips until confluence and divided into four groups: 1) Vehicle, 2) 10 ng/ml SP, 3) 10 ng/ml SP plus 10^{-7} M CBD, and 4) 10 ng/ml SP with 10^{-7} M CBD plus 9 nM GW9662 antagonist PPAR- γ . Cells were then fixed for 10 min in 4% formaldehyde, washed with ice-cold PBS and permeabilized with 0.3% Triton-X100 in PBS for 15 min. Subsequently, 2% BSA was used to block the nonspecific binding sites. The cells were then incubated overnight with mouse monoclonal anti-ZO-1 (1:100 v/v) or rabbit polyclonal antioccludin antibody

(1:100 v/v) (Table 2), following PBS washing and further incubated in the dark for half an hour with the appropriate secondary antibody FITC-conjugated antirabbit or Texas red conjugated antimouse) in the presence of DAPI as a marker of cellular nuclei. After final PBS washing, the cells were analyzed using an inverted immunofluorescence microscope (HBO fluorescence microscope IM-3FL4, Optika Microscope, Bergamo, Italy), and images were captured by a high-resolution digital camera (HDML 4083.13-ext 12 V 2000 mA, Optika Microscopes, Bergamo, Italy).

2.8 | ELISA assay for TNF- α , IL-6, IL-1 β , and IL-18 release quantification

ELISA for human TNF- α (sensitivity: 1.7 pg/ml assay range: 15.6–1,000 pg/ml), IL-6 (sensitivity: 2 pg/ml assay range: 16–1,690 pg/ml), IL-1 β (sensitivity: 2 pg/ml assay range: 33–1,400 pg/ml), and IL-18 (sensitivity: 6.25 pg/ml assay range: 25.6–1,000 pg/ml) (Thermo Fisher Scientific Inc. [Monza, Italy]) were carried out with undifferentiated Caco-2 cell supernatant after treatments at 24 h according to the manufacturer's protocol. Absorbance was measured on a microtiter plate reader. TNF- α , IL-6, IL-1 β , and IL-18 levels were thus determined using the standard curves method, respectively.

2.9 | Statistical analysis

Results are expressed as the mean \pm SD of the mean of $n = 6$ experiments in triplicate. Statistical analyses were performed using unpaired *t*-test and one-way analysis of variance (ANOVA), and multiple comparisons were performed using a Bonferroni post-hoc test. $p < 0.05$, $p < 0.01$, and $p < 0.001$ was considered to indicate a statistically significant difference.

3 | RESULTS

3.1 | Cannabidiol decreases SARS-CoV-2 spike (S) protein induced cytotoxicity and pyroptosis extent in cultured Caco-2 cells acting at PPAR- γ site

The incubation with increasing concentration (0.1–10 ng/ml) of SP caused a concentration-dependent decrease of cell viability (–21%, –47% and –72% vs. vehicle group, respectively) at 24 h in cultured Caco-2 cells by MTT analysis (Figure 1a). In the same experimental condition, SP promoted a parallel formation of pyroptotic bodies, increasing chromatin thickening in the cell nuclei (+307%, +603%, +826% vs. vehicle group) (Figure 1b,c). In the presence of CBD (10^{-9} – 10^{-7} M), a significant and concentration-dependent rescue of cell viability was obtained (+31, +110% and +214% vs. SP 10 ng/ml group), respectively (Figure 1a). In parallel with this, cannabidiol also induced a significant reduction of condensed nuclei (–20%, –36%, –68% vs. SP 10 ng/ml group) (Figure 1b,c). Interestingly, in the presence of PPAR- γ antagonist

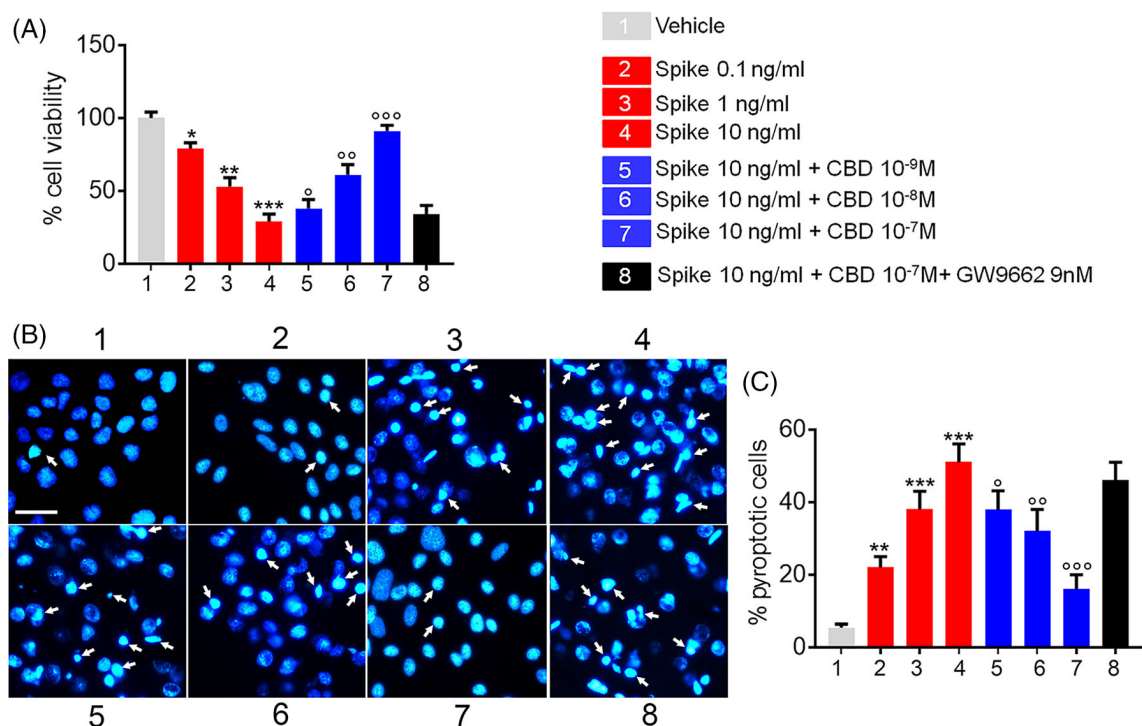


FIGURE 1 Effect of cannabidiol (CBD) on cell viability and apoptosis rate induced by severe acute respiratory syndrome by coronavirus type 2 (SARS-CoV-2) spike (S) protein challenge in Caco-2 cells. (a) MTT-formazan assay determining the quantification of cell viability in treated Caco-2 cells exposed to spike protein (SP) (0.1–10 ng/ml) in the presence of CBD (10⁻⁹–10⁻⁷ M) in the presence/absence of PPAR- γ antagonist GW9662 (9 nM) at 24 h; (b) immunofluorescence microphotographs showing 4',6-diamidino-2-phenylindole (DAPI) staining of Caco-2 cell nuclei exposed to SP (0.1–10 ng/ml) in the presence of CBD (10⁻⁹–10⁻⁷ M); and (c) quantification of the relative proportion (%) of apoptotic nuclei evidenced by chromatin aggregates (indicated by white arrows). Magnification 20 \times (scale bar, 20 μ m). Results are expressed as mean \pm standard deviation (SD) of $n = 4$ experiments performed in triplicate. *** $p < 0.001$ ** $p < 0.01$ and * $p < 0.05$, respectively, versus vehicle; ^{oo} $p < 0.001$, ^o $p < 0.01$, and ^o $p < 0.05$, respectively, versus SP 10 ng/ml

GW9662 (9 nM), the protective effect of CBD (10⁻⁷ M) both on cell viability and on pyroptotic bodies formation induced by SARS-CoV-2 SP was almost completely inhibited (Figure 1a–c).

3.2 | Cannabidiol reduces spike protein-induced ACE-2 expression and inhibits inflammasome pathway by modulating TLR4/NLRP3 protein through a PPAR- γ involvement

Following 24 h SP (0.1–10 ng/ml) incubation, a significant and concentration-dependent increase of TLR4 (+52%, +207%, +451% vs. vehicle, respectively) and ACE-2 protein expression in Caco-2 in cellular membrane homogenates was observed (+42%, +102%, +259% vs. vehicle, respectively). While on the contrary, SP caused a marked decrease of RhoA GTP (–30%, –55%, –84% vs. vehicle group, respectively) in the cytoplasmic cellular portion of Caco-2 (Figure 2a–d). In parallel with these results, SP also increased NLRP3 (+80%, +264%, and +494% vs. vehicle group, respectively) and Caspase-1 (+111%, +365% and +809% vs. vehicle, respectively) cytoplasmic protein expression in Caco-2 homogenates (Figure 2a, e, f). CBD effect resulted in a significant and concentration-dependent inhibition of both TLR4 (–28%, –41%, –76% respectively vs. SP

10 ng/ml group) and ACE-2 protein expression (–25%, –38.4%, and –57% vs. SP 10 ng/ml group) paralleled to a marked rescue of RhoA GTP (+83%, +365% and +490% vs. SP 10 ng/ml) expression (Figure 2a–d). Notably, CBD effect was thus accompanied to a significant and concentration-dependently inhibition of both NLRP3 (–22.6%, –48% and –72% vs. SP 10 ng/ml group, respectively) and Caspase-1 (–22%, –49%, –74% vs. SP 10 ng/ml group, respectively) protein expression induced by SP challenge (Figure 2a, e, f). In the same experimental conditions, as seen with regard to cytotoxicity and apoptosis experiments, in the presence of PPAR- γ antagonist GW9662 (9 nM), CBD (10⁻⁷ M) effect on protein expression modulation was almost completely abolished (Figure 2a–f).

3.3 | CBD decreases TNF- α , IL-6, IL-1 β , and IL-18 release in SP-challenged Caco-2 cells

As a consequence of proinflammatory signaling pathway activation, SP (0.1–10 ng/ml) challenge resulted in a marked increase of TNF- α (+125%, +213%, +400% vs. vehicle group, respectively), IL-6 (+144%, +217%, +337% vs. vehicle group, respectively), IL-1 β (+167%, +257%, +448% vs. vehicle group, respectively), and IL-18 (+203%, +303%, +502% vs. vehicle group, respectively) secretion in Caco-2 cell

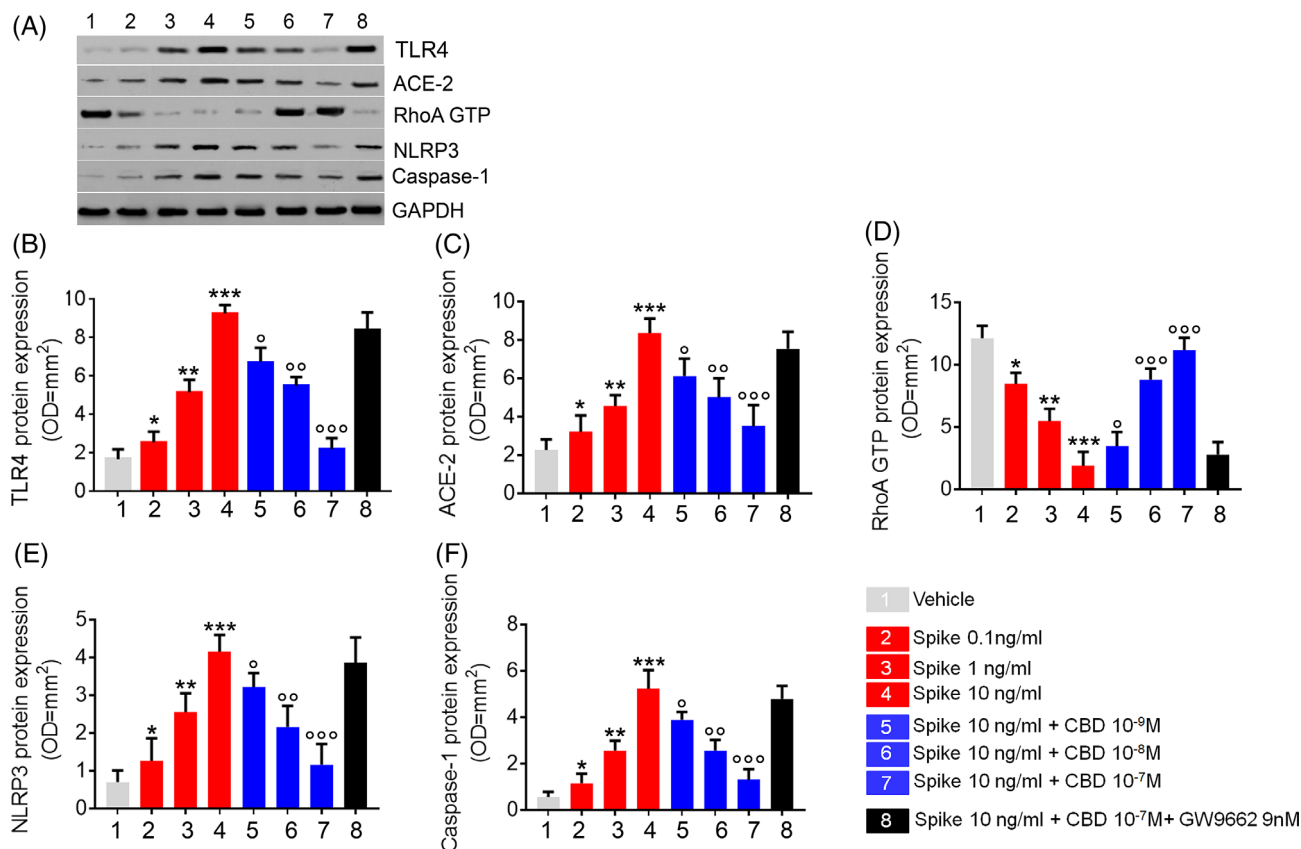


FIGURE 2 Effect of cannabidiol (CBD) (10^{-9} – 10^{-7} M) in the presence/absence of PPAR- γ antagonist GW9662 (9 nM) on ACE-2, RhoA GTPase, and TLR4/NLRP3/Caspase-1 pathway induced by spike protein (SP) (0.1–10 ng/ml) in Caco-2 cells. (a) Immunoreactive bands referred to TLR4, angiotensin converting enzyme 2 (ACE-2), RhoA GTPase, NLRP3, and Caspase-1 protein expression and (b–f) relative densitometric analysis of each protein (arbitrary units normalized on the expression of the housekeeping protein GAPDH). Results were expressed as mean \pm standard deviation (SD) of $n = 6$ experiments performed in triplicate. *** $p < 0.001$ ** $p < 0.01$, and * $p < 0.05$, respectively, versus vehicle; °°° $p < 0.001$, °° $p < 0.01$, and ° $p < 0.05$, respectively, versus SP 10 ng/ml

supernatant at 24 h (Figure 3a–d). Such observed release of proinflammatory cytokines was concentration-dependently mitigated by CBD (10^{-9} – 10^{-7} M) incubation, that resulted in a marked decrease of TNF- α (–28%, –46%, and –66% vs. SP 10 ng/ml group, respectively), IL-6 (–18%, –33%, and –65% vs. SP 10 ng/ml group, respectively), IL-1 β (–28%, –51.2% and –69% vs. SP 10 ng/ml group, respectively), and IL-18 (–29%, –49.5%, –68.10% vs. SP 10 ng/ml group, respectively) release in cell medium, reinforcing the evidence for its anti-inflammatory effect in vitro. As expected, in the presence of PPAR- γ antagonist GW9662 (9 nM), CBD (10^{-7} M) incubation did not reach any significant inhibitory effect of SARS-CoV-2 SP-induced proinflammatory cytokine release in the same experimental conditions (Figure 3a–d).

3.4 | Cannabidiol inhibits spike protein-induced epithelial damage rescuing tight junction occludin and ZO-1 expression

Following SP challenge (10 ng/ml), a significant and time-dependent reduction of TEER was observed starting from 3 h and in the subsequent time intervals at 6, 9, 12, 15, 18, 21, and 24 h in confrontation

with the vehicle group. TEER values were progressively decreased in the time by –24.2%, –33%, –50%, –64%, –78%, –80%, –81%, and –89%, respectively, versus the vehicle group (Figure 4a). In the presence of highest CBD at highest concentration (10^{-7} M), a significant rescue (+44%, +85%, +151%, +291%, +330% +363%, and +727%, respectively, versus SP 10 ng/ml group, respectively) of TEER was observed starting at 6 h in the same interval time (Figure 4a). In agreement with these results, SP (0.1–10 ng/ml) stimulus, caused a concentration-dependent increase of FITC-dextran flux in cultured cells as marker of cell permeability (+116%, +285%, +411% vs. vehicle group, respectively) (Figure 4b). According to TEER, SP effects on FITC-dextran flux were massively and concentration-dependently counteracted by CBD (–17%, –39%, and –50% vs. SP 10 ng/ml group, respectively) (Figure 4b). As expected, neither significant recovery of TEER decrease nor FITC-dextran fluxes were obtained in the same experimental conditions when CBD was co-incubated with PPAR- γ antagonist GW9662 (9 nM) (Figure 4a, b). Furthermore, immunofluorescence analysis of tight junction proteins, occludin and ZO-1, was in line with TEER data, since SP stimulus (10 ng/ml) markedly reduced both occludin (–71% vs. vehicle group) and ZO-1 (–72% vs. vehicle group) expression in cultured cells at

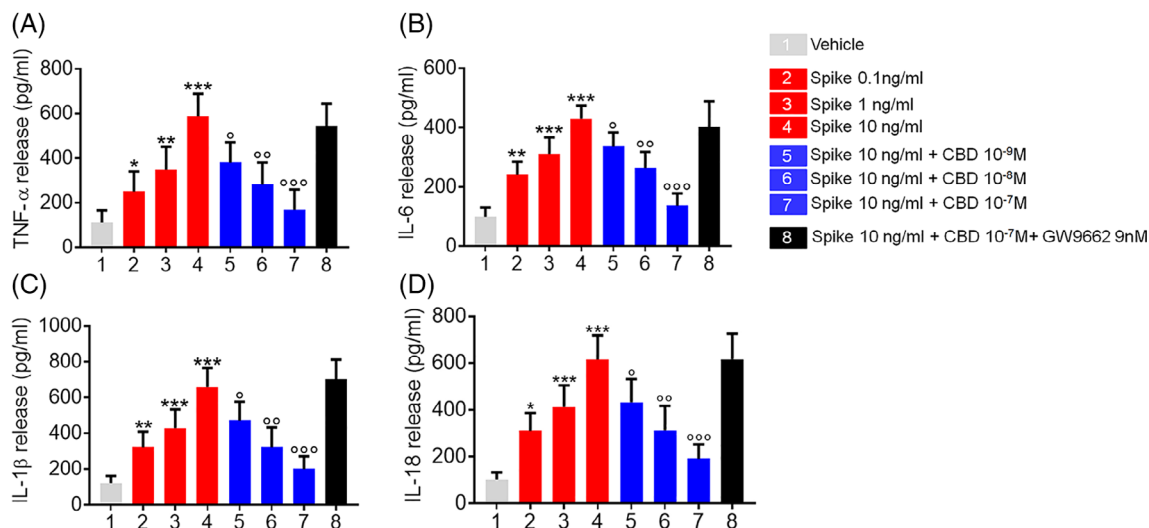


FIGURE 3 Effect of cannabidiol (CBD) (10^{-9} – 10^{-7} M) in the presence/absence of PPAR- γ antagonist GW9662 (9 nM) on (a) tumor necrotic factor alpha (TNF- α), (b) interleukin (IL)-6, (c) IL-1 β , and (d) IL-18 release in spike protein (SP) challenged Caco-2 cells. Results are expressed as mean \pm standard deviation (SD) of $n = 4$ experiments performed in triplicate. *** $p < 0.001$ ** $p < 0.01$ and * $p < 0.05$, respectively, versus vehicle; °°° $p < 0.001$, °° $p < 0.01$, and ° $p < 0.05$, respectively, versus SP 10 ng/ml

24 h (Figure 4c, d). CBD (10^{-7} M) markedly counteracted occludin (+210% vs. SP 10 ng/ml group) and ZO-1 (+150% vs. SP 10 ng/ml group) reduction, and its effect was dependent upon PPAR- γ involvement, since no protective effect on tight junction recovery was obtained in the presence of GW9662 (9 nM), once again confirming the inescapable role of this receptor in mediating CBD protection in our experimental conditions (Figure 4c, d).

4 | DISCUSSION

Although the typical manifestations of COVID-19 have been described at the pulmonary and vascular level, many patients infected with SARS-CoV-2 develop gastrointestinal symptoms, such as nausea, vomiting, and diarrhea (Ong & Dan, 2021).

Nowadays, the role of the ACE-2 receptor as the interaction site between SARS-CoV-2 SP and the host cells is well known. Intestinal epithelium, expressing significant levels of ACE-2 protein, represents a potential site of entry for SARS-CoV-2 that can allow its replication and propagation. Interestingly, the more the SARS-CoV-2 viral infection involves the intestinal epithelium, the more severe the pulmonary and postinfectious consequences of COVID-19 seem to be (Ahlawat & Sharma, 2020). As well as in the respiratory tract, Carnevale et al. hypothesized that the SARS-CoV-2 SP could play a crucial role in activating the mechanisms of epithelial damage at the intestinal mucosa site through the induction of a hyper-inflammatory status. (Carnevale et al., 2021). In the present study, we demonstrated such a theory showing that the SARS-CoV-2 SP was able to cause direct damage in Caco-2 epithelial cells in vitro. Since they can reproduce the morphology and the characteristic permeability of intestinal epithelium (Xiaomeng et al., 2021), both undifferentiated and differentiated Caco-2 epithelial cells were used to evaluate the inflammatory

response triggered by SP. In our experimental condition, SARS-CoV-2 SP incubation determined a significant increase of both TLR-4 and ACE-2 proteins expression, promoting a marked inflammatory response enhanced by the NLRP3/Caspase-1 pathway activation. These observations had also been confirmed by a marked release of proinflammatory cytokines IL-6, TNF- α , each well-known downstream product of TLR-4 activation. Also, we observed an overrelease of proinflammatory/proapoptotic mediators such as IL-1 β and IL-18 by challenged epithelial cells. These consequences of NLRP3/Caspase-1 inflammasome complex activation triggered a massive reduction of cells viability in the SP treated group, probably as the outcome of the aforementioned pro-pyoptotic mediators' over-release. Moreover, following the SP challenge in vitro, we further detected a huge ablation of RhoA GTPase and the subsequent significative loss of epithelial integrity, highlighted by the progressive reduction of TEER scores and also featured by tight junction proteins ZO-1 and occludin decrease. Such evidence demonstrated a direct enterotoxic and proinflammatory action of SARS-CoV-2 SP in vitro in our experimental conditions.

On the other hand, our results showed the PPAR- γ /concentration-dependent in vitro efficacy of CBD in controlling the inflammation through down-regulation of the NLRP3/Caspase-1 response triggered by SP stimulus. In line with various experimental evidence that has, in different conditions of cellular stress (Sunda & Arowolo, 2020), clarified how CBD determines (a) cytoprotective activity at the epithelial level preventing cells death, (b) significant reduction of inflammatory mucosal damage, and (c) recovery of transmembrane resistance values (TEER), cannabidiol treatment resulted in a marked rescue of ZO-1 and occludin expression in challenged cells, with a consistent reduction of SARS-CoV-2 Spike SP-induced cell-to-cell leakage. The present results are also in line with other studies that have shown how, beyond its marked anti-inflammatory activity

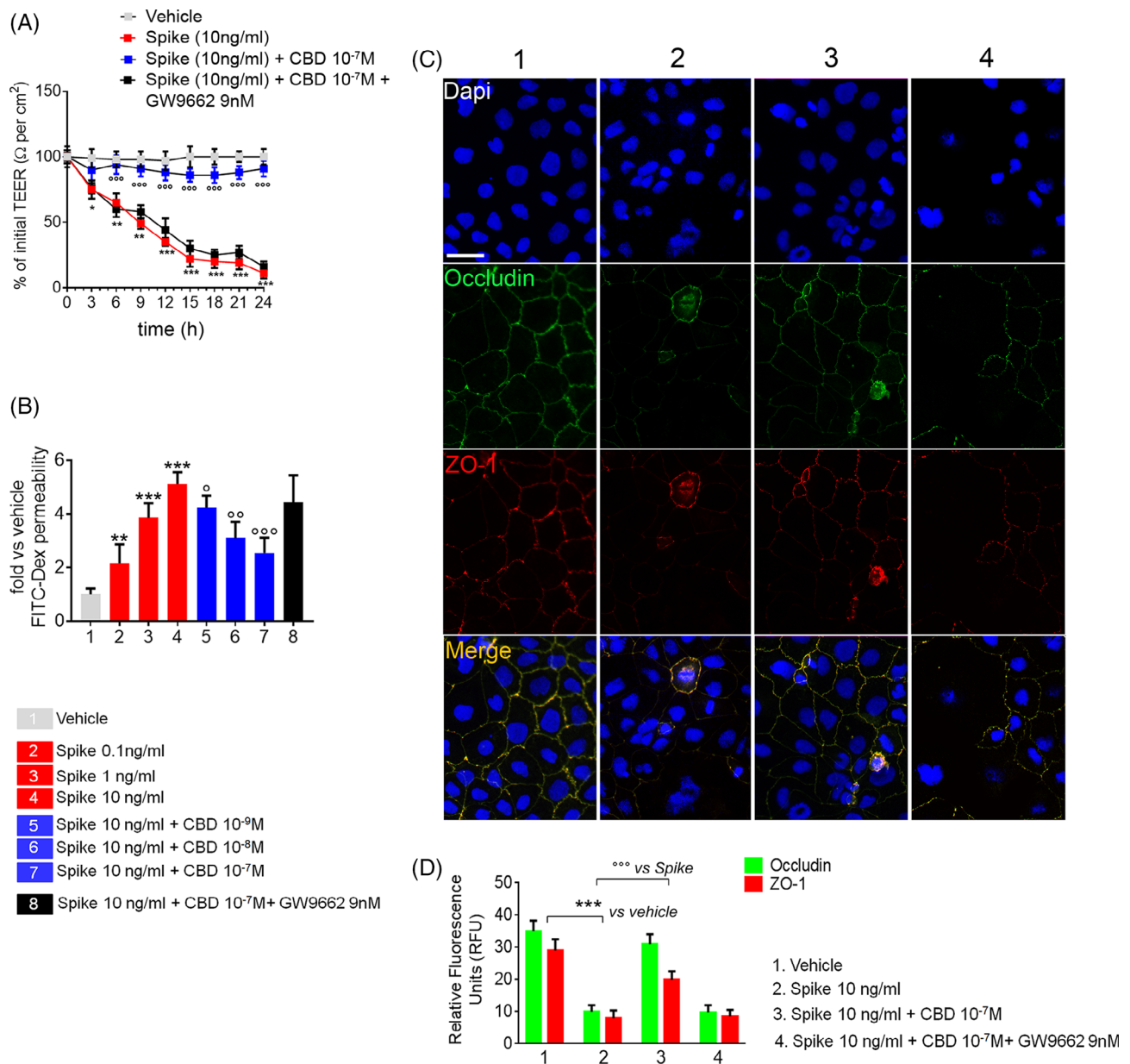


FIGURE 4 Synoptic framework showing the effect of cannabidiol (CBD) alone or in the presence of PPAR- γ antagonist GW9662 (9 nM) on electric resistance, FITC-dextran flux leakage, and barrier integrity of Caco-2 cells exposed to spike protein (SP). (a) Time course of transepithelial electrical resistance (TEER) changes; (b) cell permeability measured by FITC-dextran flux leakage after 24 h of treatment; (c) immunofluorescent staining showing occludin (green) and zonula occludens-1 (ZO-1) (red) co-expression after 24 h of treatment, and (d) relative occludin and ZO-1 quantification by relative fluorescence units (RFU). Immunofluorescent staining showing occludin (green) and ZO-1 (red) co-expression after 24 h of treatment. Nuclei were stained by 4',6-diamidino-2-phenylindole (DAPI). Magnification $20\times$ (scale bar = 25 μm). Results are expressed as mean \pm standard deviation (SD) of $n = 4$ experiments performed in triplicate. *** $p < 0.001$, ** $p < 0.01$, and * $p < 0.05$, respectively, versus vehicle; $^{\circ\circ\circ}p < 0.001$, $^{\circ\circ}p < 0.01$, and $^{\circ}p < 0.05$, respectively, versus SP 10 ng/ml

(Nelson et al., 2020), CBD might exert a remarkable gate-keeper capacity on the intestinal epithelium (Berg et al., 2021). This CBD's efficacy in counteracting the induced cell damage and epithelial hyperpermeability has been highlighted in several models, ranging from bacterial toxins (Joffre et al., 2020) to other stimuli (Cocetta et al., 2021).

Interestingly, we noticed that the reduction of cells viability was almost the same in the group treated with the specific PPAR- γ inhibitor

GW9662 (8) and in the one treated with SP ng/ml (4). In parallel, the groups treated with CBD, without GW9662 (5-7), showed a significant and concentration-dependent rescue of cells viability. These experimental outcomes suggested that CBD, acting at the PPAR- γ site, can interfere with inflammasome complex formation, preventing the release of proapoptotic mediators and rescuing cells viability (Yang et al., 2021). Moreover, in our experimental conditions, CBD incubation was able to down-regulate the expression of the ACE-2 receptor in

Caco-2 cells. Interestingly, a previous study by Anil group observed a similar decrease of the ACE-2 receptor in lung epithelial cells induced by CBD (Anil et al., 2021). This combined preliminary evidence may suggest that such a molecule could systemically reduce the patient's susceptibility to SARS-CoV-2 infection. Also, patients expressing high ACE-2 density seem to be more susceptible to SARS-CoV-2 and to show worse clinical outcomes. Conversely, healthy patients with much lower activity for this receptor have beneficial anti-inflammatory, antioxidant and antifibrotic effects (Malinowska et al., 2021).

Molecules capable of reducing the hyperinflammatory response that characterizes the most severe clinical forms of COVID-19 are strategically essential in supporting therapies against SARS-CoV-2 infections. Such molecules can significantly reduce the damage deriving from the cytokine storm and might strongly reduce the need for intensive care units for the most compromised patients. CBD is suitable for this purpose, and if orally administered, as the antiepileptic CBD-based drug Epidiolex, it demonstrated itself capable of reducing the susceptibility caused by SARS-CoV-2 (Nguyen et al., 2021). Moreover, as an anti-inflammatory and immunoregulatory agent, CBD has shown the therapeutic potential of certain advantages in controlling the picture of lung inflammation from COVID-19 and proving capable of markedly improve the symptoms of SARS-CoV-2 infection-mimicking model by poly (I: C)-induced ARDS (Khodadadi et al., 2020) in mice. Moreover, CBD demonstrated itself capable of increasing the expression of apelin, a peptide with a significant role in the central and peripheral regulation of the immune system, CNS, metabolic, and cardiovascular system. These effects, added to its known anti-inflammatory properties identified at the lung level, are in line with other preclinical models of ARDS (Ribeiro et al., 2012; Salles et al., 2020). In this sense, acting at the PPAR- γ site, CBD has been proposed as a drug of potential applicability in anti-COVID-19 protocols, as demonstrated by an increasing number of clinical trials that examine its protective effect in SARS-CoV-2 infections (NCT04731116; NCT04686539). In addition to these previous publications, our study first demonstrates, as far we know, new and potential effects of CBD in the intestinal epithelium, potentially able to counteract SARS-CoV-2 hyper-inflammation in the gut. We consider this point extremely interesting since the emerging importance of the intestine in viral replication, especially for SARS-CoV-2 variants (Du et al., 2020), the role exerted by intestinal mucosa in the immune response to viral attack mediated by SP in this site. Although our data refer to an *in vitro* model, and further *in vivo* investigations are needed, they indicate additional potential beneficial effects by CBD against COVID-19 that integrate with previously established lung protection. Moreover, by reducing ACE-2 expression and down-regulating RhoA-GTPase/NLRP3/Caspase-1 pathway, by a selective PPAR- γ involvement, CBD may potentially counteract viral entry and replication by the intestine. At the same time, this molecule can reduce the over-release of proinflammatory cytokine at the basis of systemic inflammatory dysfunction in most severe COVID-19 cases (Esposito, Pesce, Seguella, Sanseverino, Lu, Corpetti, et al., 2020a).

A possible critical point in CBD use in COVID-19 patients is the possible interaction of this molecule with current COVID-19 therapies. We can hypothesize that the *in vitro* inhibitory propriety of CBD

on CYP450 (Millar et al., 2019) may increase plasma concentrations of other medications. Luckily, considering that the CBD concentration required (IC50) to inhibit CYP450 is significantly higher than the cannabidiol plasma concentration achieved by o.s. (as well as the one used in our experimental conditions), we do not expect serious side effects at usually therapeutical CBD doses.

In conclusion, if CBD effects, here reported, will be confirmed *in vivo*, we could have more information about the effective protective potential of CBD not only restricted at the pulmonary level. Future studies are needed to consolidate our *in vitro* data in *in vivo*, in a model of intestinal SARS-CoV-2 SP-induced damage. Also, additional investigations will be able to clarify the consequences of ACE-2 down-regulation and the impact of this in susceptibility to SARS-CoV-2. In perspective, this could imply that a CBD-mediated defence against COVID-19 at the gastrointestinal tract would result in a possible control of the SARS-CoV-2 enteral route of infection. In theory, thus, the restoration of the mucosal permeability exerted by CBD would allow a possible inhibition of a pathway involved in the amplification of the SARS-CoV-2 infection toward the lung or CNS (Peyravian et al., 2020), beneficially impacting the clinical worsening and severity of COVID-19 course observed in so many patients.

ACKNOWLEDGMENTS

The assistance of the staff is gratefully appreciated. Open Access Funding provided by Universita degli Studi di Roma La Sapienza within the CRUI-CARE Agreement. [Correction added on 23 June 2022, after first online publication: CRUI funding statement has been added.]

FUNDING

The present experimental work was partially supported by SAPIENZA University Grants n. AR11816433B8F7F8 assigned to Luisa Seguella.

CONFLICT OF INTEREST

The authors declare that the research was conducted in the absence of any commercial or financial relationships that could be construed as a potential conflict of interest.

AUTHOR CONTRIBUTIONS

Chiara Corpetti, Giuseppe Esposito, and Giovanni Sarnelli conceived the project and performed the experiments, Alessandro Del Re, Giovanni Sarnelli, Luisa Seguella, and Marcella Pesce helped with the experiments and critically analyzed the obtained experimental data; Sara Rurgo, Barbara De Conno, and Irene Palenca were also involved in cell culture and immunofluorescence analysis data elaboration. Alessandro Del Re, Chiara Corpetti, and Giuseppe Esposito wrote the manuscript. Chiara Corpetti and Marcella Pesce contributed to the critical revision of the manuscript. Irene Palenca edited the manuscript and helped to perform the statistical analysis of the data. Giovanni Sarnelli and Giuseppe Esposito were responsible for the overall project conception and development. All the authors discussed the results and commented on the manuscript. The authors read and approved the final manuscript.

DATA AVAILABILITY STATEMENT

The raw data supporting the conclusions of the present manuscript will be made available by the authors, without undue reservation.

ORCID

Marcella Pesce  <https://orcid.org/0000-0001-5996-4259>

Giuseppe Esposito  <https://orcid.org/0000-0001-8080-8218>

REFERENCES

- Ahlatwaj, S. A., & Sharma, K. K. (2020). Immunological co-ordination between gut and lungs in SARS-CoV-2 infection. *Virus Research*, 286, 198103. <https://doi.org/10.1016/j.virusres.2020.198103>
- Alhaboruni, A., Lee, A. C., Wright, K. L., Larvin, M., & O'Sullivan, S. E. (2010). Pharmacological effects of cannabinoids on the Caco-2 cell culture model of intestinal permeability. *The Journal of Pharmacology and Experimental Therapeutics*, 335(1), 92–102. <https://doi.org/10.1124/jpet.110.168237>
- Anil, S. M., Shalev, N., Vinayaka, A. C., Nadarajan, S., Namdar, D., Belausov, E., ... Koltai, H. (2021). Cannabis compounds exhibit anti-inflammatory activity in vitro in COVID-19-related inflammation in lung epithelial cells and pro-inflammatory activity in macrophages. *Scientific Reports*, 11(1), 1462. <https://doi.org/10.1038/s41598-021-81049-2>
- Berg, B. B., Soares, J. S., Paiva, I. R., Rezende, B. M., Rachid, M. A., Cau, S. B. A., ... Castor, M. (2021). Cannabidiol enhances intestinal cannabinoid receptor type 2 receptor expression and activation increasing regulatory T cells and reduces murine acute graft-versus-host disease without interfering with the graft-versus-leukemia response. *The Journal of Pharmacology and Experimental Therapeutics*, 377(2), 273–283. <https://doi.org/10.1124/jpet.120.000479>
- Bifulco, M., Fiore, D., Piscopo, C., Gazzerò, P., & Proto, M. C. (2021). Commentary: Use of cannabinoids to treat acute respiratory distress syndrome and cytokine storm associated with coronavirus disease-2019. *Frontiers in Pharmacology*, 12, 631646. <https://doi.org/10.3389/fphar.2021.631646>
- Carnevale, S., Beretta, P., & Morbini, P. (2021). Direct endothelial damage and vasculitis due to SARS-CoV-2 in small bowel submucosa of COVID-19 patient with diarrhea. *Journal of Medical Virology*, 93(1), 61–63. <https://doi.org/10.1002/jmv.26119>
- Chung, J. Y., Thone, M. N., & Kwon, Y. J. (2021). COVID-19 vaccines: The status and perspectives in delivery points of view. *Advanced Drug Delivery Reviews*, 170, 1–25. <https://doi.org/10.1016/j.addr.2020.12.011>
- Cocetta, V., Governa, P., Borgonetti, V., Tinazzi, M., Peron, G., Catanzaro, D., ... Montopoli, M. (2021). Cannabidiol isolated from *Cannabis sativa* L. protects intestinal barrier from in vitro inflammation and oxidative stress. *Frontiers in Pharmacology*, 12, 641210. <https://doi.org/10.3389/fphar.2021.641210>
- De Filippis, D., Esposito, G., Cirillo, C., Cipriano, M., De Winter, B. Y., Scuderi, C., ... Iuvone, T. (2011). Cannabidiol reduces intestinal inflammation through the control of neuroimmune axis. *PLoS One*, 6(12), e28159. <https://doi.org/10.1371/journal.pone.0028159>
- Del Re, A., Corpetti, C., Pesce, M., Seguela, L., Steardo, L., Palencia, I., ... Esposito, G. (2021). Ultramicrosized palmitoylethanolamide inhibits NLRP3 inflammasome expression and pro-inflammatory response activated by SARS-CoV-2 spike protein in cultured murine alveolar macrophages. *Metabolites*, 11, 592. <https://doi.org/10.3390/metabo11090592>
- Dickson, I. (2020). Organoids demonstrate gut infection by SARS-CoV-2. *17(7)*, 383–383.
- Du, P., Song, C., Li, R., Song, Y., Li, J., Ding, N., ... Zeng, H. (2020). Specific re-distribution of SARS-CoV-2 variants in the respiratory system and intestinal tract. *Clinical Infectious Diseases*. <https://doi.org/10.1093/cid/ciaa1617>
- Esposito, G., Pesce, M., Seguela, L., Sanseverino, W., Lu, J., Corpetti, C., & Sarnelli, G. (2020a). The potential of cannabidiol in the COVID-19 pandemic. *British Journal of Pharmacology*, 177(21), 4967–4970. <https://doi.org/10.1111/bph.15157>
- Esposito, G., Pesce, M., Seguela, L., Sanseverino, W., Lu, J., & Sarnelli, G. (2020b). Can the enteric nervous system be an alternative entrance door in SARS-CoV2 neuroinvasion? *Brain, Behavior, and Immunity*, 87, 93–94. <https://doi.org/10.1016/j.bbi.2020.04.060>
- Gigli, S., Seguela, L., Pesce, M., Bruzzese, E., D'Alessandro, A., Cuomo, R., ... Esposito, G. (2017). Cannabidiol restores intestinal barrier dysfunction and inhibits the apoptotic process induced by *Clostridium difficile* toxin A in Caco-2 cells. *United European Gastroenterology Journal*, 5(8), 1108–1115. <https://doi.org/10.1177/2050640617698622>
- Izzo, A. A., & Sharkey, K. A. (2010). Cannabinoids and the gut: New developments and emerging concepts. *Pharmacology & Therapeutics*, 126(1), 21–38. <https://doi.org/10.1016/j.pharmthera.2009.12.005>
- Joffre, J., Yeh, C. C., Wong, E., Thete, M., Xu, F., Zlatanova, I., ... Hellman, J. (2020). Activation of CB(1)R promotes lipopolysaccharide-induced IL-10 secretion by monocytic myeloid-derived suppressive cells and reduces acute inflammation and organ injury. *Journal of Immunology*, 204(12), 3339–3350. <https://doi.org/10.4049/jimmunol.2000213>
- Kelley, N., Jeltema, D., Duan, Y., & He, Y. (2019, Jul 6). The NLRP3 Inflammasome: An overview of mechanisms of activation and regulation. *International Journal of Molecular Sciences*, 20(13), 3328–3328. <https://doi.org/10.3390/ijms20133328>
- Khodadadi, H., Salles, É. L., Jarrahi, A., Chibane, F., Costigliola, V., Yu, J. C., ... Baban, B. (2020). Cannabidiol modulates cytokine storm in acute respiratory distress syndrome induced by simulated viral infection using synthetic RNA. *Cannabis and Cannabinoid Research*, 5(3), 197–201. <https://doi.org/10.1089/can.2020.0043>
- Kopel, J., Perisetti, A., Gajendran, M., Boregowda, U., & Goyal, H. (2020). Clinical insights into the gastrointestinal manifestations of COVID-19. *Digestive Diseases and Sciences*, 65(7), 1932–1939. <https://doi.org/10.1007/s10620-020-06362-8>
- Malinowska, B., Baranowska-Kuczko, M., Kicman, A., & Schlicker, E. (2021). Opportunities, challenges and pitfalls of using cannabidiol as an adjuvant drug in COVID-19. *International Journal of Molecular Sciences*, 22(4), 1986. <https://doi.org/10.3390/ijms22041986>
- Millar, S. A., Stone, N. L., Bellman, Z. D., Yates, A. S., England, T. J., & O'Sullivan, S. E. (2019). A systematic review of cannabidiol dosing in clinical populations. *British Journal of Clinical Pharmacology*, 85(9), 1888–1900. <https://doi.org/10.1111/bcp.14038>
- Mosmann, T. (1983). Rapid colorimetric assay for cellular growth and survival: application to proliferation and cytotoxicity assays. *Journal of immunological methods*, 65(1-2), 55–63. [https://doi.org/10.1016/0022-1759\(83\)90303-4](https://doi.org/10.1016/0022-1759(83)90303-4)
- Mishima, K., Hayakawa, K., Abe, K., Ikeda, T., Egashira, N., Iwasaki, K., & Fujiwara, M. (2005). Cannabidiol prevents cerebral infarction via a serotonergic 5-hydroxytryptamine1A receptor-dependent mechanism. *Stroke*, 36(5), 1077–1082. <https://doi.org/10.1161/01.Str.0000163083.59201.34>
- Nagarkatti, P., Miranda, K., & Nagarkatti, M. (2020). Use of cannabinoids to treat acute respiratory distress syndrome and cytokine storm associated with coronavirus disease-2019. *Frontiers in Pharmacology*, 11, 589438. <https://doi.org/10.3389/fphar.2020.589438>
- Nelson, K. M., Bisson, J., Singh, G., Graham, J. G., Chen, S. N., Friesen, J. B., ... Pauli, G. F. (2020). The essential medicinal chemistry of cannabidiol (CBD). *Journal of Medicinal Chemistry*, 63(21), 12137–12155. <https://doi.org/10.1021/acs.jmedchem.0c00724>
- Nguyen, L. C., Yang, D., Nicolaescu, V., Best, T. J., Ohtsuki, T., Chen, S. N., ... Rosner, M. R. (2021). Cannabidiol inhibits SARS-CoV-2 replication and promotes the host innate immune response. *bioRxiv: The Preprint Server for Biology*. <https://doi.org/10.1101/2021.03.10.432967>
- Ong, J., & Dan, Y. Y. (2021). GI-COVID: Are there COVID-19 patients with primary gastrointestinal SARS-CoV-2 infection and symptoms.

- Digestive Diseases and Sciences*, 1-3, 3228–3230. <https://doi.org/10.1007/s10620-020-06767-5>
- O'Sullivan, S. E., & Kendall, D. A. (2010). Cannabinoid activation of peroxisome proliferator-activated receptors: Potential for modulation of inflammatory disease. *Immunobiology*, 215(8), 611–616. <https://doi.org/10.1016/j.imbio.2009.09.007>
- Park, Y. H., Wood, G., Kastner, D. L., & Chae, J. J. (2016). Pyyrin inflammasome activation and RhoA signaling in the autoinflammatory diseases FMF and HIDS. *Nature Immunology*, 17(8), 914–921. <https://doi.org/10.1038/ni.3457>
- Peyravian, N., Deo, S., Daunert, S., & Jimenez, J. J. (2020). Cannabidiol as a novel therapeutic for immune modulation. *Immunotargets and Therapy*, 9, 131–140. <https://doi.org/10.2147/itt.S263690>
- Rabin Medical Center. (2021). *Cannabidiol treatment for severe and critical coronavirus (COVID-19) pulmonary infection*. ClinicalTrials.gov Identifier: NCT04731116; Rabin Medical Center; Moshe Yeshurun NCT04731116.
- Ribeiro, A., Ferraz-de-Paula, V., Pinheiro, M. L., Vitoretti, L. B., Mariano-Souza, D. P., Quinteiro-Filho, W. M., ... Palermo-Neto, J. (2012). Cannabidiol, a non-psychoactive plant-derived cannabinoid, decreases inflammation in a murine model of acute lung injury: Role for the adenosine A(2A) receptor. *European Journal of Pharmacology*, 678(1–3), 78–85. <https://doi.org/10.1016/j.ejphar.2011.12.043>
- Salles, É. L., Khodadadi, H., Jarrahi, A., Ahluwalia, M., Paffaro, V. A., Jr., Costigliola, V., ... Baban, B. (2020, Nov). Cannabidiol (CBD) modulation of apelin in acute respiratory distress syndrome. *Journal of Cellular and Molecular Medicine*, 24(21), 12869–12872. <https://doi.org/10.1111/jcmm.15883>
- Sarnelli, G., Gigli, S., Capoccia, E., Iuvone, T., Cirillo, C., Seguella, L., Nobile, N., D'Alessandro, A., ... Esposito, G. (2016). Palmitoylethanolamide exerts antiproliferative effect and downregulates vegf signaling in caco-2 human colon carcinoma cell line through a selective ppar- α -dependent inhibition of akt/mTOR pathway. *Phytotherapy research: PTR*, 30(6), 963–970. <https://doi.org/10.1002/ptr.5601>
- Sebastian, J. T., Alexander, S., Christoph, K., Matthias, Z., Julia, F., Marie-Christine, A., ... Jan, R. (2021). Research Square <https://doi.org/10.21203/rs.3.rs-30407/v1>
- Sheba Medical Center. (2020). *Synthetic CBD as a Therapy for COVID-19*. ClinicalTrials.gov Identifier: NCT04686539; Sheba Medical Center NCT04686539.
- Sunda, F., & Arowolo, A. (2020). A molecular basis for the anti-inflammatory and anti-fibrosis properties of cannabidiol. *The FASEB Journal*, 34(11), 14083–14092. <https://doi.org/10.1096/fj.202000975R>
- Walls, A. C., Park, Y. J., Tortorici, M. A., Wall, A., McGuire, A. T., & Velesler, D. (2020). Structure, function, and antigenicity of the SARS-CoV-2 spike glycoprotein. *Cell*, 181(2), 281–292.
- Wells, C. L., van de Westerlo, E. M., Jechorek, R. P., Haines, H. M., & Erlandsen, S. L. (1998). Cytochalasin-induced actin disruption of polarized enterocytes can augment internalization of bacteria. *Infection and Immunity*, 66(6), 2410–2419. <https://doi.org/10.1128/IAI.66.6.2410-2419.1998>
- Wu, X. X., Huang, X. L., Chen, R. R., Li, T., Ye, H. J., Xie, W., ... Cao, GZ. (2019). Paeoniflorin prevents intestinal barrier disruption and inhibits lipopolysaccharide (LPS)-induced inflammation in caco-2 cell monolayers. *Inflammation*, 42, 2215–2225. <https://doi.org/10.1007/s10753-019-01085-z>
- Xiaomeng, D., Hu, X., Chen, Y., Xie, J., Ying, M., Wang, Y., & Yu, Q. (2021). Differentiated Caco-2 cell models in food-intestine interaction study: Current applications and future trends. *Trends in Food Science & Technology*, 107, 455–465, ISSN 0924-2244. <https://doi.org/10.1016/j.tifs.2020.11.015>
- Yang, C. C., Wu, C.-H., Lin, T.-C., Cheng, Y.-N., Chang, C.-S., Lee, K.-T., ... Tsai, Y.-S. (2021). Inhibitory effect of PPAR γ on NLRP3 inflammasome activation. *Theranostics*, 11(5), 2424–2441. Published 2021 Jan 1. <https://doi.org/10.7150/thno.46873>
- Zhang, H., Kang, Z., Gong, H., Xu, D., Wang, J., Li, Z., ... Xu, H. (2020). Digestive system is a potential route of COVID-19: An analysis of single-cell coexpression pattern of key proteins in viral entry process. *Gut*, 69(6), 1010–1018. <https://doi.org/10.1136/gutjnl-2020-320953>
- Zhao, Y., Kuang, M., Li, J., Zhu, L., Jia, Z., Guo, X., ... You, F. (2021). SARS-CoV-2 spike protein interacts with and activates TLR4. *Cell Research*, 31, 818–820. <https://doi.org/10.1038/s41422-021-00495-9>

How to cite this article: Corpetti, C., Del Re, A., Seguella, L., Palencia, I., Rurgo, S., De Conno, B., Pesce, M., Sarnelli, G., & Esposito, G. (2021). Cannabidiol inhibits SARS-Cov-2 spike (S) protein-induced cytotoxicity and inflammation through a PPAR γ -dependent TLR4/NLRP3/Caspase-1 signaling suppression in Caco-2 cell line. *Phytotherapy Research*, 35(12), 6893–6903. <https://doi.org/10.1002/ptr.7302>